Photon Netw Commun (2018) 35:210–224
https://doi.org/10.1007/s11107-017-0730-z

ORIGINAL PAPER

Performance of OFDM-FSO link with analog network coding

Pravindra Kumar[1] · **Satyajit Thakor**[1]

Received: 20 December 2016 / Accepted: 5 August 2017 / Published online: 7 September 2017

Abstract Free space optical (FSO) communication link based on orthogonal frequency division multiplexing (OFDM) gives improved performance because of high bandwidth efficiency, improved robustness against fading, and narrowband interference. Any FSO system requires line-of-sight (LoS) link and in non-LoS (NLoS) situation, the two users cannot communicate directly resulting in link outage. To solve this problem, this paper proposes to use relay-assisted NLoS-FSO link with energy-saving three time-slotted analog network-coding approach to make the successful communication with increased throughput and improved error performance. The error performance of laser link is evaluated in terms of receiver sensitivity. Gamma–Gamma distribution is used for atmospheric turbulence in this analysis. The performance of relay-assisted intensity modulated/direct detected-OFDM FSO link with and without analog network coding (ANC) is compared.

Keywords OFDM system · LoS/NLoS-FSO link · Gamma–Gamma distribution · Analog network coding · MeijerG-function

1 Introduction

High speed, no electromagnetic interference (EMI), large bandwidth, unlicensed spectrum, low power requirement, high security, light weight, and low cost are some of the advantages of FSO link over radio frequency (RF) communication system. Many factors such as scattering, light reflection, atmospheric turbulence, gases, cloud cover, wind, rain, dust, fog, smoke, snow, and other non-ideal characteristics of the system can degrade the performance of FSO link [1–4]. FSO link technology was considered as a potential distributer of worldwide interoperability for microwave access (WiMAX) traffic in metro or access networks [5–9]. Cvijetic et al., in 2006, studied transmission of OFDM-WiMAX traffic over FSO link via subcarrier modulation with direct/heterodyne detection in [6,7], respectively, where outage and symbol error performance was determined for both detection techniques. In 2006 [8], a multiple-input–multiple-output (MIMO) architecture for distributing WiMAX traffic using optical wireless technology is presented, where different protocols are considered. In 2008 [9], the 10 Gb/s first experimental demonstration of OFDM-FOS link is given in the presence of atmospheric effects, including variable power attenuation and signal fading. N. Zdravkovi et al., in 2016, presented outage analysis of Mixed FSO/WiMAX Link in [10]. A. Bekkali et al. [11], in 2010, presented the closed-form expressions for the OFDM-based turbulent radio-over-FSO (RoFSO) system and studied the transmission performance of the link. M. Sharma et al. [12,13], in 2013 and 2014, have evaluated the capacity of MIMO-OFDM FSO communication system in the presence of intersymbol interference (ISI) for different values of weak atmospheric turbulence strength and studied the performance of spatially multiplexed MIMO-OFDM FSO communication system. The transmission performance of OFDM FSO system using dual-diversity reception under correlated lognormal distribution have studied by F. Bai et al. [14] in 2014. The theoretical reference to study coherent detection OFDM-FSO systems was given by Y. Wang et al. [15], in 2015. P. Kumar et al. [16], in 2015, compared the performance of OFDM and TDM

✉ Pravindra Kumar
ait.pravs@gmail.com; pravindra_k@students.iitmandi.ac.in

Satyajit Thakor
satyajit@iitmandi.ac.in

[1] School of Computing and Electrical Engineering, Indian Institute of Technology, Mandi, H.P. 175001, India

signals over unlicensed turbulent FSO link. In 2016, the performance of multi-user OFDM-FSO link was improved with combined receive space diversity and transmit frequency diversity [17]. In OFDM-FSO link with individual orthogonal subcarriers, the multiple independent subsignals for main signal are modulated and multiplexed in RF domain. This RF-OFDM signal is converted into optical OFDM signal using laser diode (LD) and transmitted to the turbulent FSO channel. At the receiver end, this optical signal is received by photodetector (PD) diode that uses direct detection technique. The complex equalization is not required due to less distortion experienced in OFDM-FSO link [18]. Due to the saving in electrical bandwidth, ease of channel and phase estimation, and scalability to higher-order modulation [19], OFDM is used for FSO link in this paper.

In RF systems, the OFDM signal is bipolar and complex which cannot be applied to the LD because it cannot generate intensity variation for negative amplitude signals. Thus a positive and real RF-OFDM signal is required for IM/DD systems. To generate positive and real signal, there are different techniques used in the literature [20–29]: DCO-OFDM [20]; ACO-OFDM [21,22]; combined asymmetrically clipped-DC-biased optical OFDM (ADO-OFDM) [23]; hybrid ACO-OFDM [24]; asymmetrically and symmetrically clipping optical OFDM (ASCO-OFDM) [25]; auto-bias controlled technique [26]; optimal DC-biasing for DCO-OFDM [27]. In DCO-OFDM technique, DC bias is applied to make the entire negative part of the signal positive. If sufficient DC bias is not added, the remaining negative part of the signal gets clipped and results in clipping noise. With DC bias addition, the average OFDM signal power is increased and that leads to enhancement in nonlinearity effects at the transmitter and optical channel. Thus, DCO-OFDM is not a power-efficient technique. ACO-OFDM is a power-efficient technique where additional DC bias to make the OFDM signal positive is not required. In ACO-OFDM, the complex symbols are mapped only on the odd subcarriers, whereas even subcarriers are set to zero. The generated bipolar signal is then clipped at zero to make it positive. This positive signal is only applied to the laser for direct detection. The clipping does not introduce any loss of information due to anti-symmetric property of ACO-OFDM. S. D. Dissanayak et al. [23], J. Armstrong et al. [28], D. Patel et al. [29], compared the performance of DCO-OFDM and ACO-OFDM and have shown that ACO-OFDM provides better system performance for short distance up to 75 km. ACO-OFDM using 16-QAM has the same normalized bandwidth as DCO-OFDM using 4-QAM but requires 4.7 dB less power than DCO-OFDM with 7 dB bias. In DCO-OFDM, the optimum value of DC bias depends on the QAM constellation. Large constellations would require more DC bias to eliminate the clipping noise. L. Chen et al. [30] characterized the nonlinear biasing and clipping effects on an IM/DD optical OFDM system. They have shown that nonlinear clipping distortion process can be modeled as a virtual relay channel. This nonlinear process can be modeled as a linear deterministic attenuation plus an uncorrelated random additive clipping noise in the time domain.

In FSO channel, scattering due to fog creates multiple propagation paths resulting in multiple reception of the transmitted signal. Due to multiple reception, temporal broadening (dispersion) of the transmitted signal arises, which creates ISI resulting into performance degradation [31–33]. This dispersion is linear distortion in the channel, but it is converted into nonlinear distortion after square-law-based detection at the receiver. This nonlinear distortion can reduce the effectiveness of linear equalization. The square-root-module (SRM) device, added after photodiode detector to compensate for square-law behavior, improves linear equalizer performance resulting in overall performance improvement of OFDM-FSO link [34–36].

An FSO system, based on line-of-sight (LoS), is concerned with the transmission of optical beam carrying information through free space. If there is obstacle between the users, then an event of link outage occurs. In this non-LoS (NLoS) situation, users cannot communicate directly with each other. To make possible the information exchange, a relay can be used, and with it, both the users can communicate with each other, and this scheme is known as traditional scheme (TS) [37]. The capacity or throughput or achievable rate of TS link is less since more time slots are required to make a end-to-end communication. To improve the information rate in relay network, various coding schemes are used such as digital network coding (DNC), analog network coding (ANC), physical layer network coding (PLNC) scheme, in RF-wireless communication system [37].

1.1 Related work

FSO systems with network coding have been studied in related works [38–42]. The related work [37] of S. C. Liew et al. gives an overview of PLNC, TC, DNC, and ANC schemes with an example where PLNC scheme can improve throughput by 100% in passive optical network (PON). In wireless communication networks, to prevent harmful interference, scheduling of multiple transmission at the same time is avoided. Instead of avoiding interference, PLNC scheme exploits the use of interference to increase the network capacity. The related work [43] of S. Katti et al. proposed and implemented ANC, a less complex version of PLNC, where the received mixed signal at the relay is simply amplified and forwarded without any processing. In [37], the achievable rates, in symmetric exchange rates, of PLNC, DNC, ANC, and TS under equal power usages for all nodes are compared and it has been shown that PLNC performs better with high achievable rate as compared to other schemes. The related work [44,45] of H. Gacanin et al. and T. Sjodin et al., give the study of OFDM link based on ANC with the perfect knowledge of channel state information. However, this ANC scheme cannot exploit the direct link between the two users, i.e., LoS link, even if it exists physically resulting in poorer performance despite of having high spectral efficiency and diversity. A three time-slotted analog network coding (3T-ANC) scheme has been proposed [46–49] that can utilize the direct link by allowing the transmission of two users in two different time slots and the relay transmission in third time slot. Consequently, the 3T-ANC scheme can improve the performance of a two-way relay channel in presence of direct LoS link.

1.2 Our contribution

In all related works [37,43–45], a network coding scheme (such as DNC, ANC, and PLNC) is applied in wireless communication networks and have shown that PLNC performed better than ANC scheme, but, in optical communication point-of-view, PLNC is not cost efficient. In this work, the performance of OFDM-based FSO link, with various network coding schemes, is analyzed to make successful end-to-end communication with increased capacity of the link. In addition to this, we analyze the performance of ANC scheme in FSO network where both NLoS and LoS link are present at the same time. Normally ANC scheme is based on amplify-forward (AF) protocol with two time slot requirement for delivering the end-to-end information resulting into increased capacity of relay-assisted FSO link. In presence of both NLoS and LoS link in FSO network, we propose to use three time-slotted ANC scheme referred to as 3T-ANC scheme that can gives further improvement in receiver sensitivity and increase throughput of FSO link.

In ANC, the relay operation is based on AF protocol and in PLNC, the relay operation is based on decode-forward (DF) protocol resulting into reduced cost and complexity with ANC scheme as compared to PLNC scheme. ANC, with no optical-to-electrical (O/E) and electrical-to-optical (E/O) conversion for AF operation at relay, consumes less electrical power than PLNC where E/O and O/E is mandatory during DF operation at relay. Thus, ANC is energy- and cost- saving approach in communication network because it minimizes the number of optical–electrical–optical (O/E/O) conversion interface and electrical interface resulting into less energy consumption at the relay.

In this work, we have compared the performance of ACO-OFDM and DCO-OFDM FSO link in LoS situation. Also we have compared the ACO-OFDM and DCO-OFDM in NLoS+LoS with 3T-ANC scheme. The new results show that with 3T-ANC scheme, the ACO-OFDM technique is also power-efficient scheme where additional DC bias is not required to make the RF-OFDM signal positive.

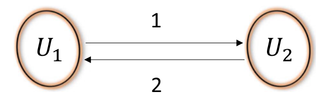

Fig. 1 Two-way network (without relay)

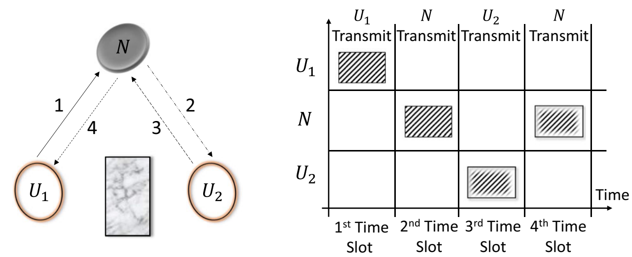

Fig. 2 A two-way relay network (TWRN) or traditional scheme (TS)

The performance of OFDM-FSO link with different network coding schemes over turbulent FSO channel is compared in terms of achievable rate vs SNR and BER vs received power. In this work, Gamma-Gamma distribution is used to describe turbulent-induced-faded atmospheric channel. The paper is organized as follows: Various network coding schemes with 3T-ANC scheme are described in Sect. 2. The architecture of OFDM transmitter and receiver for optical signal transmission and reception over turbulent FSO link and FSO channel model is discussed in Sect. 3. The achievable rate and BER analysis are discussed in Sect. 4. Results are discussed in Sect. 5, and finally the conclusion is given in Sect. 6.

2 Network coding

2.1 Digital network coding

Consider a situation as shown in Fig. 1, where two users U_1 and U_2 wants to communicate each other via an FSO link. If the channel is half duplex and LoS event occurs, then two stages are required to exchange information between them.

In a situation when an obstacle is between them, communication link will breakdown. To solve this problem, relay-assisted NLoS-FSO link can be used where the relay N is added to facilitate communication as shown in Fig. 2. This kind of network is known as two-way relay network (TWRN), and this scheme is known as traditional scheme (TS) [37]. In this condition, four stages are required instead of two as in LoS situation, and hence, with this, there is 50% degradation in throughput.

In TS, to avoid interference, the signals transmitted form U_1 and U_2 are separated in time or wavelength. If the relay is capable of mixing the two data packets together, the four time slots needed in TS to exchange information is reduced to three

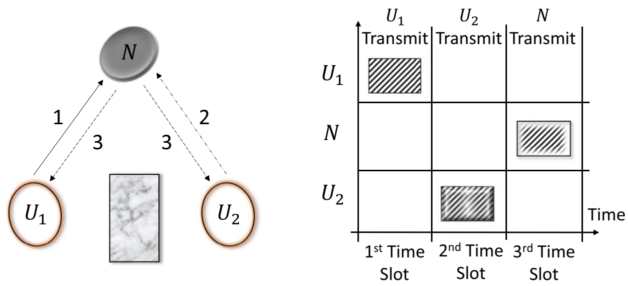

Fig. 3 Digital network coding (DNC)-based two-way relay network

time slots as shown in Fig. 3. This TS with mixing capable relay is known as DNC scheme. Thus, DNC has throughput improvement of 33% over TS or DNC has a coding gain of 1.3. In this, users U_1 and U_2 transmit their packets P_1 and P_2 during the first and second time slots, respectively. The relay receives data packets and performs XOR operation bitwise, i.e., $P_{1,2} = f(P_1, P_2) = P_1 \oplus P_2$ (thus encodes two packets into one) and then broadcast it to both the users during third time slot. In DNC, the decode-forward operation is done at the relay, and thus O/E/O conversion is required at the relay.

For simplicity, assume that users U_1 and U_2 transmits bits 0 and 1 during the first and second time slots, respectively. Relay perform XOR operation on bit 0 and 1 to create a mixed bit $(0 \oplus 1 = 1)$. This bit 1 is broadcasted. Now, at user end U_1, XOR operation is performed on received broadcasted bit and transmitted bit itself i.e., $(1 \oplus 0 = 1)$. Thus, U_1 will receive successfully the transmitted bit by U_2. With this same procedure U_2 can also recover the transmitted bit by user U_1. Thus, in DNC scheme, users transmit sequentially, the relay mixes the content of the packets and broadcasts the mixed version.

Note that, both TWRN without network coding and with DNC, avoid simultaneous transmissions i.e., different time slots are for each user. After receptions at the relay, network coding is performed.

2.2 Physical layer network coding (PLNC)

In PLNC, only two time slots are required as compared to three time slots required in DNC scheme. In the first time slot, users U_1 and U_2 transmit their data to relay N. Based on the superimposed EM waves that carry packets of U_1 and U_2, i.e., P_1 and P_2, respectively, relay N computes $P_{1,2} = P_1 \oplus P_2$. In the second time slot, relay N broadcasts the $P_{1,2}$ to both the users. Thus, there is 100% improvement in throughput of canonical relay network. The signal broadcasted in second time slot in PLNC is the same as the signal transmitted in third time slot in DNC. The key difference of the two systems lies in how they derive $P_{1,2}$. In DNC, P_1 and P_2 are separately transmitted by users U_1 and U_2; and relay N decodes P_1 and P_2 in order to form $P_{1,2}$. In PLNC, $P_{1,2}$ is derived from $P_1 + P_2$, which is the superimposed signal received in the first time slot. The superimposed signal is due to the network coding performed by nature and the relay transforms it to the XOR network coding function, i.e., $P_{1,2} = f(P_1, P_2)$. At both users, U_1 and U_2, there must be a network decoding functions g_1 and g_2, such that $P_2 = g_1(f(P_1, P_2), P_1)$ and $P_1 = g_2(f(P_1, P_2), P_2)$, to extract their counterpart's signal from $P_{1,2}$ and self-information. PLNC can be divided into two types [50] based on whether the range of f is a finite or infinite set. Finite set PLNC include the XOR operation and known as simple PLNC; on the other hand, infinite set PLNC is known as ANC in which the relay N retains the additive mixing that occurs in the nature and amplifies the simultaneously received signals and noise and then broadcast it to both the users. In the case of ANC, the received signal is $R_s = f(S_1, S_2) = h_1 S_0 + h_2 S_1$, where h_1 and h_2 are the channel fading coefficients between user U_1 to relay N and U_2 to the relay N, S_1 and S_2 are the transmitted signals from user U_1 and U_2 to relay, respectively. In PLNC, DF operation is also performed at the relay, thus in case of FSO link, O/E/O conversion is also required at the relay that can increase the cost and complexity of the relay significantly.

2.3 Analog network coding (ANC)

Instead of avoiding interference at the relay, ANC utilizes it. The relay forwards received mixed signals, and the destinations use their information to cancel the self-interference and thus recover the desired signal. ANC is less complex version of PLNC, since the relay uses AF instead of DF protocol [37,43–45]. The difference between ANC and PLNC, in optical communication point-of-view, is as follows: (1) ANC is based on AF protocol where the interfering signal of both the users by the channel is simply amplified with the help of optical amplifier, i.e., EDFA and forwarded to both the users. On the other hand, PLNC is based on DF protocol where the received signals from both the users is decoded and converted into bits and after applying XOR operation it is forwarded to both the users; (2) optical amplifier can directly amplify the optical signal without O/E conversion, and thus, there is no need for O/E/O conversion at the relay resulting into lower complexity and cost of the relay-assisted link. On the other hand, O/E/O conversion is required at the relay in PLNC, and thus, relay is equipped with both electrical and optical components resulting into higher complexity and cost of the relay-assisted link. The relay that require O/E/O conversion can be termed as opto-electronic relay (OER), and the relay without this requirement termed as optical relay (OR) ; (3) because of only EDFA at relay, ANC scheme consume less electrical power, whereas PLNC scheme consumes higher electrical power because of decoding operation and

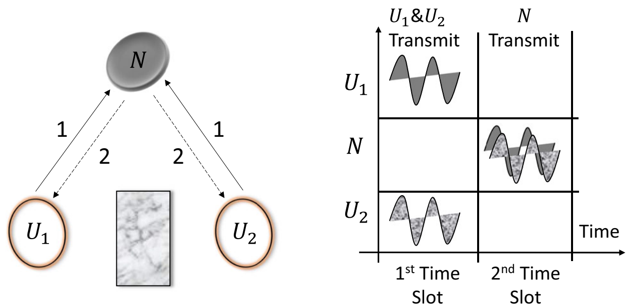

Fig. 4 Analog network coding (ANC)-based two-way relay network

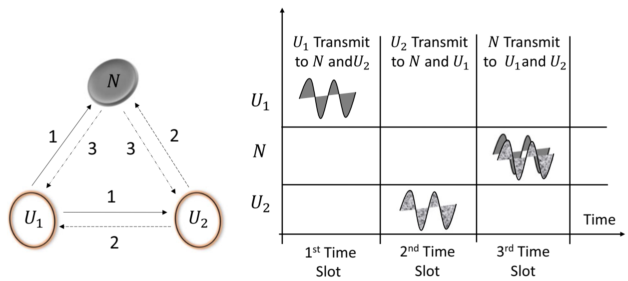

Fig. 5 Three time-slotted analog network coding (3T-ANC)

O/E/O conversion at the relay; (4) ANC performs AF operation on signals not on bits. On the other hand, PLNC performs decode-forward operation on bits not signals; (5) finite-field mapping is used in PLNC, whereas infinite-field mapping is used in ANC [50]; (6) PLNC is used when the uplink is good and ANC is used when downlink is good [37,50].

ANC scheme is shown in Fig. 4, where two time slots are required to exchange information between two users. The first time slot is used by both users simultaneously to transmit their signals to the relay and this stage is termed as multiple access (MA) stage. The combined signal at the relay is broadcasted in second time slot, and this stage is termed as and termed as broadcast channel (BC) stage.

2.4 Three time-slotted ANC (3T-ANC) scheme

The 3T-ANC scheme is shown in Fig. 5, where three time slots are needed. In the first time slot, user U_1 broadcasts its signal to both relay N and node U_2. In the second time slot, user U_2 broadcasts its signal to both relay N and node U_1. In the third time slot, relay N broadcasts its combined amplified signal back to the users. The protocol for 3T-ANC has been investigated in [47].

2.5 Mathematical model for ANC and 3T-ANC

Consider a two user nodes U_1- and U_2-based FSO system consisting an amplify-forward (AF) relay node N as shown

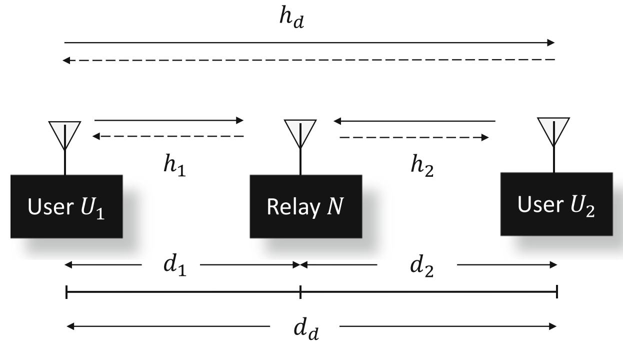

Fig. 6 A relay-assisted FSO system model

in Fig. 6. The turbulent-induced faded atmospheric channels between the nodes are described by Gamma–Gamma distribution, and they are time invariant during transmission phases. Let h_d and h_j are the channel fading coefficients of direct LoS link between U_1 and U_2 at distance d_d, and the relay link between U_j to N at distance d_j for $j = 1, 2$.

In ANC scheme, users U_j transmit their OFDM signal $S_j(t)$ in first time slot simultaneously for $j = 1, 2$. The received signals at relay node N is given as

$$R_{N,1}(t)^{\mathrm{ANC}} = \sum_{j=1}^{2} h_j S_j(t) + n_{N,1}(t). \tag{1}$$

It is noticeable here that a user cannot receive the signal from other during the first time slot.

In the second time slot, the transmitted relay signal, with transmit power P_N, to both of the users is given as

$$T_{N,2}(t)^{\mathrm{ANC}} = G_2 R_{N,1}(t)^{\mathrm{ANC}}. \tag{2}$$

where G_2 is the amplifying gain factor.

The signal received at U_j in the second time slot is given as

$$R_{U_j,2}(t)^{\mathrm{ANC}} = h_j G_2 \left(h_1 S_1(t) + h_2 S_2(t) + n_{N,1}(t)\right) + n_{U_j,2}(t). \tag{3}$$

After self-interference $(G_2 h_j h_j S_j(t))$ cancelation, the received signal is given as

$$R_{U_j,2}(t)^{\mathrm{ANC}} = G_2 h_j h_i S_i(t) + G_2 h_j n_{R,1}(t) + n_{U_j,2}(t). \tag{4}$$

where $(i, j) = (1, 2), (2, 1)$, $n_{k,j} \sim N(0, \sigma^2)$ is the additive noise at node k in the jth time slot, $\sim$ stands for 'distributed as', $N(0, \sigma^2)$ denotes the zero mean Gaussian distribution with σ^2 variance. Finally, user U_j detects the signal of user U_i from $r_{U_j,2}(t)^{\mathrm{ANC}}$.

In 3T-ANC, three time slots are required in completing the information exchange: user U_j broadcast their OFDM signal $S_j(t)$ in the jth time slot for $j = 1, 2$, and the relay N broadcast their signal $S_3(t)$ in the third time slot. The received signals, in the first time slot, at the relay node N and at user node U_2 are given as

$$R_{N,1}(t)^{\text{3T-ANC}} = h_1 S_1(t) + n_{N,1}(t). \quad (5)$$
$$R_{U_2,1}(t)^{\text{3T-ANC}} = h_d S_1(t) + n_{U_2,1}(t). \quad (6)$$

Similarly, the received signals at the relay node N and at user node U_1 in the second time slot are given as

$$R_{N,2}(t)^{\text{3T-ANC}} = h_2 S_2(t) + n_{N,2}(t). \quad (7)$$
$$R_{U_1,2}(t)^{\text{3T-ANC}} = h_d S_2(t) + n_{U_1,2}(t). \quad (8)$$

The relay signal, in the third time slot, is linear combination of two received signals and can be given as

$$S_3(t)^{\text{3T-ANC}} = G_3 \left\{ R_{N,1}(t)^{\text{3T-ANC}} + R_{N,2}(t)^{\text{3T-ANC}} \right\}. \quad (9)$$

where G_3 is the amplifying gain factor.

The signal received at node U_j in the third time slot is given as

$$R_{U_j,3}(t)^{\text{3T-ANC}} = G_3 h_j \left\{ h_i S_i(t) + h_j S_j(t) + (n_{N,1} + n_{N,2}) \right\} + n_{U_j,3}. \quad (10)$$

After self-interference elimination, the received signal at node U_j is given as

$$R_{U_j,3}(t)^{\text{3T-ANC}} = G_3 h_j h_i S_i(t) + G_3 h_j \left(n_{N,1} + n_{N,2} \right) + n_{U_j,3}. \quad (11)$$

for $(i, j) = (1, 2), (2, 1)$. Now, this received signal is combined with Eq. (6) for $j = 2$ and Eq. (8) for $j = 1$ as the direct received signal is available. Performing the maximal ratio combining (MRC), the resultant end-to-end SNR from U_i to U_j can be obtained.

2.6 Multiple relay-assisted FSO link

To further improve the receiver sensitivity and achievable rate of 3T-ANC-based FSO link, one can use more than one relay nodes between two source nodes. A two-way relay FSO channel with n relay nodes is shown in Fig. 7. The combination of FSO link with multi-relay networks is termed as co-operative FSO (C-FSO) communication system which can be a promising technique to achieve the power reduction objective, since it could be used to enhance the system throughput and increase the coverage area without increasing transmission power.

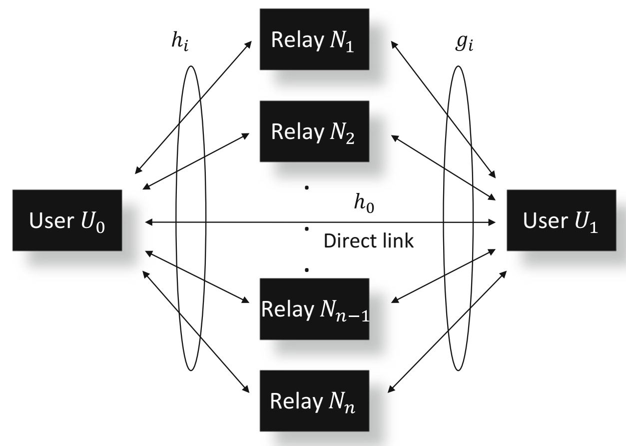

Fig. 7 C-FSO link with multiple relay

3 System and channel model

3.1 Architecture of OFDM transmitter and receiver

The transmitter (Tx) and receiver (Rx) architecture are shown in Figs. 8 and 9. At the transmitter, after inverse fast Fourier transform (IFFT) and cyclic prefix (CP) addition, the time domain RF-OFDM signal is obtained. The CP addition helps to remove intercarrier interference and intersymbol interference. The optical OFDM signal is obtained, after parallel-to-serial (P/S) and digital-to-analog converter (DAC), using LD and Mach–Zehnder modulator (MZM) at optical transmitter [19]. This optical signal is transmitted through the FSO channel using FSO transmit antenna. At the receiver, the optical signal is converted into RF signal using photodetector [51]. The received signal is sampled with analog-to-digital converter (ADC). After S/P, fast Fourier transform (FFT), 4-QAM demodulation and finally P/S converter, the transmitted signal is recovered back. The orthogonality allows the use of FFT to reconstruct the transmitted signal at the receiver side and requires simple equalization [18].

The time domain RF-OFDM signal is defined as

$$\mathrm{S}_j(t) = \sqrt{P} \sum_{k=0}^{N_{\mathrm{sc}}-1} \mathrm{s}_j(k) e^{j2\pi f_k t}; \quad j = 1, 2. \quad (12)$$

where $\mathrm{S}_j(t)$ is the OFDM signal of user U_j, $P (= \frac{E_s}{T_c N_{\mathrm{sc}}})$ is the power coefficient, N_{sc} is the total number of subcarriers. E_s is the data-modulated symbol energy, T_c is the sampling period, f_k should be equal to $\frac{k-1}{T_s}$ to maintain the orthogonality between subcarriers, T_s is OFDM symbol duration and s_k is data symbol of kth subcarrier.

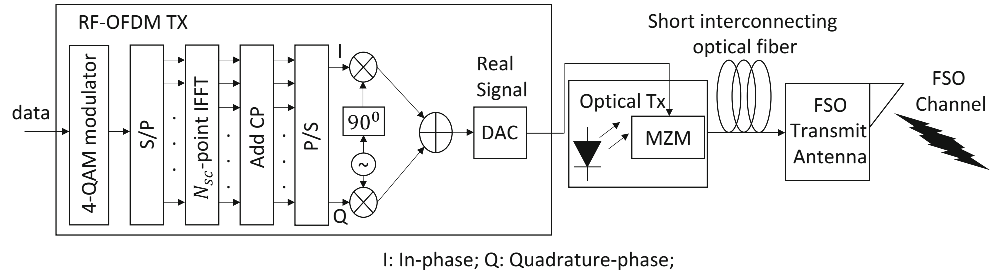

Fig. 8 Block diagram of OFDM transmitter architecture [17]

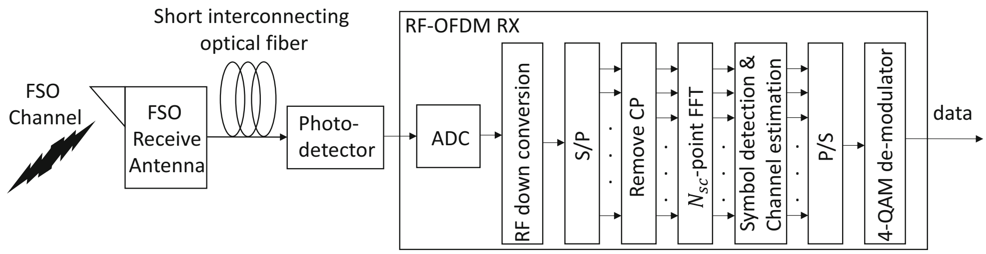

Fig. 9 Block diagram of OFDM receiver architecture [17]

The OFDM signal $\mathrm{S}_j(t)$ is used to modulate the optical intensity of LD and transmitted through FSO channel. The laser optical power output from LD is given as [11,52]

$$P_{\mathrm{T}}(t) = P_{\mathrm{av}} n_{\mathrm{T}} G_{\mathrm{T}} \times \left[1 + m\,\mathrm{S}_j(t)\right] \cos(2\pi \nu t). \tag{13}$$

where P_{av} is the average transmitted optical power, G_{T} is the transmitter antenna gain, n_{T} is the optical transmitter efficiency, ν is the optical carrier frequency and m is the modulation index.

The Friis transmission equation is used to define the received optical power by PD diode and can be given as [51]

$$P_{\mathrm{R}}(t) = P_{\mathrm{T}}(t) n_{\mathrm{R}} G_{\mathrm{R}} \left(\frac{\lambda}{4\pi L}\right)^2 \times 10^{(-\delta L/10)}. \tag{14}$$

where n_{R} is the optical receiver efficiency, $G_{\mathrm{R}} \left(= \left(\frac{\pi D_{\mathrm{r}}}{\lambda}\right)^2 \right)$ is the gain of receiver antenna and D_{r} is the receiver collecting lens aperture diameter.

The diode current can be obtained by putting Eq. (13) into Eq. (14) and is given as [11,52]

$$i(t) = \Re G n_{\mathrm{T}} n_{\mathrm{R}} G_{\mathrm{T}} G_{\mathrm{R}} P_{\text{T-av}} \left(\frac{\lambda}{4\pi L}\right)^2 \times 10^{(-\delta L/10)} \times [1 + m\, S(t)] \cos(2\pi \nu t) + n_{\mathrm{opt}}. \tag{15}$$

where $\Re$ is the photodetector responsivity, G is the optical amplifier gain, n_{opt} is the dominant noise present in the FSO communication laser link which is combination of relative intensity noise, thermal noise, and shot noise [53].

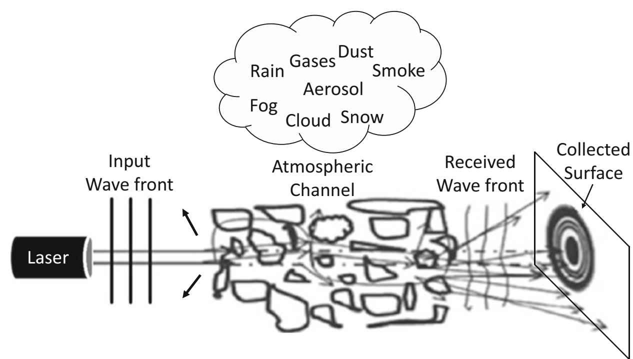

Fig. 10 FSO channel model

The bandwidth for OFDM signal is given as [19] $B_{\mathrm{OFDM}} = \frac{2}{T_s} + \frac{N_{\mathrm{sc}}-1}{t_s}$, where t_s is observation time of IFFT window. For a data rate of 1 Gb/s, $\frac{1}{9}$ overhead of CP, 110 data, and 18 pilot subcarriers, the required bandwidth of OFDM signal per user is 0.586 GHz. For TDM case, the required bandwidth, with 1 Gb/s data rate, is approximately 1 GHz. Thus, compared to TDM system, there is 41.4% reduction in required bandwidth with OFDM system.

3.2 FSO channel characteristics

Figure 10 shows the statistical FSO channel model, where the laser signal transmission is affected by atmospheric losses (due to show, rain, fog etc.,), pointing losses, atmospheric turbulence, background noise or ambient light, beam divergence, and optical/window losses. The forward error correcting codes (turbo codes, LDPC), high transmit power, adaptive optics, MIMO, multi-beam hybrid FSO/RF system, and optical/electrical filtering help to mitigate adverse effect due to these factors. The eye safety due to laser radiation in FSO link is another challenge that can cause damage to eye and skin. The system can be within eye safety limit with operating it 1550 nm wavelength range and/or using class-1 laser.

The atmospheric turbulent channel, where the channel fading coefficient is multiplied by optical signal, can be characterized by multiplicative noise and defined as

$$R = hS + n. \tag{16}$$

where R and S are the received and transmitted signals, respectively, h is the channel fading coefficient and n is additive white Gaussian noise (AWGN) with σ^2 variance.

The channel fading coefficient h consists the effect of varying weather condition such as rain, fog, snow, gases, etc., with creates atmospheric attenuation (h_a), and varying refractive index of air i.e., atmospheric turbulence which creates scintillation (h_s). Thus, $h = h_a h_s$ and the Beer Lambert law is used to calculate the value of $h_a (= e^{-\delta L})$ [54], where δ is atmospheric attenuation coefficient defined by Kim model [55].

In modeling of optical channel, the Gamma–Gamma distribution is used for accurate estimation of probability density function (pdf) of the random signal [54], where the channel state h_s described as

$$f_{h_s}(h_s) = \frac{2(\alpha\beta)^{\frac{\alpha+\beta}{2}}}{\Gamma(\alpha)\Gamma(\beta)} h_s^{\frac{\alpha+\beta}{2}-1} K_{\alpha-\beta}\left(2\sqrt{\alpha\beta h_s}\right). \tag{17}$$

where $h_s > 0$, $K_n(.)$ is the second kind nth-ordered modified Bessel function, $\Gamma(.)$ is the Gamma function, α and β are the scintillation parameters defined for spherical wave as [54]

$$\alpha = \left[\exp\left\{\frac{0.49\beta_0^2}{\left(1+0.56\beta_0^{12/5}\right)^{7/6}}\right\} - 1\right]^{-1}, \tag{18}$$

$$\beta = \left[\exp\left\{\frac{0.51\beta_0^2}{\left(1+0.69\beta_0^{12/5}\right)^{5/6}}\right\} - 1\right]^{-1}. \tag{19}$$

where $\beta_0^2 \left(= 0.5C_n^2 k^{7/6} L^{11/6}\right)$ is the Rytov variance for spherical wave, $C_n^2 \left(m^{-2/3}\right)$ is the refractive index structure parameter and $k = 2\pi/\lambda$ is the optical wave number.

The pdf of channel state h, with the deterministic nature of atmospheric attenuation h_a, is given as [54]

$$f_h(h) = \left|\frac{\mathrm{d}}{\mathrm{d}h}\left(\frac{h}{h_a}\right)\right| f_{h_s}\left(\frac{h}{h_a}\right). \tag{20}$$

According to [56, Eq. (03.04.26.0008.01)], the modified Bessel function (in Eq. (17)) in terms of MeijerG-function is $K_n(X) = \frac{1}{2} G_{0,2}^{2,0}\left(\frac{X^2}{4}\middle|_{\frac{n}{2},-\frac{n}{2}}^{-}\right)$. Thus, from Eqs. (17) and (20), the pdf of channel state h is defined as

$$f_h(h) = \frac{(\alpha\beta)^{\frac{\alpha+\beta}{2}} h^{\frac{\alpha+\beta}{2}-1}}{\Gamma(\alpha)\Gamma(\beta) h_a^{\frac{\alpha+\beta}{2}}} G_{0,2}^{2,0}\left(\alpha\beta\frac{h}{h_a}\middle|_{\frac{\alpha-\beta}{2},\frac{\beta-\alpha}{2}}^{-}\right). \tag{21}$$

4 Achievable rate and bit error rate (BER)

4.1 Achievable rate

Let $C_{j\longrightarrow N}$ be the uplink information capacity from node j to relay N and $C_{N\longrightarrow j}$ be the downlink information capacity from relay N to node j. Thus, information capacity is given as

$$\begin{aligned} C_{j\longrightarrow N} &= \tfrac{1}{2}\log_2\left(1 + \tfrac{P_{\mathrm{R}_{j\longrightarrow N}}}{\sigma^2}\right), \\ C_{N\longrightarrow j} &= \tfrac{1}{2}\log_2\left(1 + \tfrac{P_{\mathrm{R}_{N\longrightarrow j}}}{\sigma^2}\right). \end{aligned} \tag{22}$$

where $P_{\mathrm{R}_{j\longrightarrow N}}$ is the received power by relay N from node j and $P_{\mathrm{R}_{N\longrightarrow j}}$ is the received power by node j from relay N, for $j = 1, 2$.

Let $t_{\mathrm{MA}} \geq 0$ be the fraction of time used in MA time slot during which the relay receives from user U_j and $t_{\mathrm{BC}} = 1 - t_{\mathrm{MA}}$ the fraction of time used in BC time slot during which the relay transmit to user U_j. The information rate from user U_1 to user U_2 and from user U_2 to user U_1 can be given as

$$\begin{aligned} \c{C}_{1\longrightarrow 2}(t_{\mathrm{MA}}) &= \min\left[t_{\mathrm{MA}} C_{1\longrightarrow R}, \quad t_{\mathrm{BC}} C_{R\longrightarrow 2}\right], \\ \c{C}_{2\longrightarrow 1}(t_{\mathrm{MA}}) &= \min\left[t_{\mathrm{MA}} C_{2\longrightarrow R}, \quad t_{\mathrm{BC}} C_{R\longrightarrow 1}\right]. \end{aligned} \tag{23}$$

To achieve symmetry for achievable rates in both direction, i.e., $\c{C}_{1\longrightarrow 2} = \c{C}_{2\longrightarrow 1}$, homogeneous scenario is considered in which the same transmit power with same channel gains is used by both users and relay i.e., $P_{j\longrightarrow N} = P_{N\longrightarrow j} = P_N = P$.

In LoS scheme, two time slots are needed with same amount of time in each transmission. Thus, the achievable rate can be given as [37]

$$\begin{aligned} \c{C}^{\mathrm{LoS}}_{1\longrightarrow 2} = \c{C}^{\mathrm{LoS}}_{2\longrightarrow 1} &= \tfrac{1}{2} \times \tfrac{1}{2}\log_2\left(1 + \tfrac{P}{\sigma^2}\right) \\ &= \tfrac{1}{4}\log_2\left(1 + \mathrm{SNR}^{\mathrm{LoS}}_{i\longrightarrow j}\right). \end{aligned} \tag{24}$$

With LoS scheme, this is an upper bound on achievable rates.

In TS scheme with link-by-link channel coding, four time slots are needed with same amount of time in each transmission. Thus, the quarter of the airtime is used in each transmission, and the achievable rate can be given as

$$\begin{aligned} \varsigma^{\text{TS}}_{1\longrightarrow 2} = \varsigma^{\text{TS}}_{2\longrightarrow 1} &= \frac{1}{4} \times \frac{1}{2}\log_2\left(1+\frac{P}{\sigma^2}\right) \\ &= \frac{1}{8}\log_2\left(1+\text{SNR}^{\text{TS}}_{i\longrightarrow j}\right). \end{aligned} \quad (25)$$

In DNC, each transmission requires three time slots of same amount. Thus, the achievable rate can be given as

$$\begin{aligned} \varsigma^{\text{DNC}}_{1\longrightarrow 2} = \varsigma^{\text{DNC}}_{2\longrightarrow 1} &= \frac{1}{3} \times \frac{1}{2}\log_2\left(1+\frac{P}{\sigma^2}\right) \\ &= \frac{1}{6}\log_2\left(1+\text{SNR}^{\text{DNC}}_{i\longrightarrow j}\right). \end{aligned} \quad (26)$$

In 3T-ANC, each transmission requires three time slots of same amount. Thus, after performing maximal ratio combining (MRC) technique, SNR from U_i to U_j can be given as [49].

$$\begin{aligned} \text{SNR}^{\text{3T-ANC}}_{i\longrightarrow j} &= P_{i\longrightarrow j}\frac{|h_d|^2}{\sigma^2} + \frac{G_3^2 P_{i\longrightarrow N}|h_i|^2\left|h_j\right|^2}{G_3^2\left|h_j\right|^2\sigma^2+\sigma^2} \\ &= P_{i\longrightarrow j}\alpha_d + \frac{G_3^2 P_{i\longrightarrow N}|h_i|^2\left|h_j\right|^2}{G_3^2\left|h_j\right|^2\sigma^2+\sigma^2}. \end{aligned} \quad (27)$$

where $\alpha_i\left(=\frac{|h_i|^2}{\sigma^2}\right)$ is the normalized SNR of link i, $G_3\left(=\sqrt{\frac{P_N}{P_{i\longrightarrow N}|h_i|^2+P_{j\longrightarrow N}\left|h_j\right|^2+\sigma^2}}\right)$ is the amplification gain factor to make the relay power P_N.

After putting the value of G_3 in Eq. (26), the end-to-end SNR is given as

$$\begin{aligned} \text{SNR}^{\text{3T-ANC}}_{i\longrightarrow j} &= P_{i\longrightarrow j}\alpha_d + \left\{\frac{G_3^2 P_{i\longrightarrow N}|h_i|^2\left|h_j\right|^2}{G_3^2\left|h_j\right|^2\sigma^2+\sigma^2}\right\} \\ &= P_{i\longrightarrow j}\alpha_d \\ &\quad + \left\{\frac{\left(\frac{P_N}{P_{i\longrightarrow N}|h_i|^2+P_{j\longrightarrow N}\left|h_j\right|^2+\sigma^2}\right)P_{i\longrightarrow N}|h_i|^2\left|h_j\right|^2}{\left(\frac{P_N}{P_{i\longrightarrow N}|h_i|^2+P_{j\longrightarrow N}\left|h_j\right|^2+\sigma^2}\right)\left|h_j\right|^2\sigma^2+\sigma^2}\right\} \\ &= P_{i\longrightarrow j}\alpha_d + \left\{\frac{P_{i\longrightarrow N}P_N\alpha_i\alpha_j}{P_{i\longrightarrow N}\alpha_i+\left(P_{j\longrightarrow N}+P_{i\longrightarrow N}\right)\alpha_j+1}\right\} \\ &= P + \frac{P^2}{3P+1}. \end{aligned} \quad (28)$$

The achievable rate can be given as

$$\varsigma^{\text{3T-ANC}}_{1\longrightarrow 2} = \varsigma^{\text{3T-ANC}}_{2\longrightarrow 1} = \frac{1}{6}\log_2\left[1+\text{SNR}^{\text{3T-ANC}}_{i\longrightarrow j}\right]. \quad (29)$$

In ANC scheme where a direct LoS is not available, end-to-end SNR can be obtained by letting $\alpha_d = 0$ in Eq. (27). Thus, the SNR from U_i to U_j for ANC scheme can be given as [37,49]

$$\begin{aligned} \text{SNR}^{\text{ANC}}_{i\longrightarrow j} &= \frac{P_{i\longrightarrow N}P_N\alpha_i\alpha_j}{P_{i\longrightarrow N}\alpha_i+\left(P_{j\longrightarrow N}+P_{i\longrightarrow N}\right)\alpha_j+1} \\ &= \frac{P^2}{3P+1}. \end{aligned} \quad (30)$$

As two time slots are required in ANC scheme, the achievable rate can be given as [37]

$$\varsigma^{\text{ANC}}_{1\longrightarrow 2} = \varsigma^{\text{ANC}}_{2\longrightarrow 1} = \frac{1}{4}\log_2\left[1+\text{SNR}^{\text{ANC}}_{i\longrightarrow j}\right]. \quad (31)$$

In PLNC scheme, two time slots are required with the same amount of time in each transmission. Thus, the achievable rate can be given as [37]

$$\varsigma^{\text{PLNC}}_{1\longrightarrow 2} = \varsigma^{\text{PLNC}}_{2\longrightarrow 1} = \frac{1}{2}\,\frac{\log_2(1+P).\log_2(1/2+P)}{\log_2(1+P)+\log_2(1/2+P)}. \quad (32)$$

4.2 Bit-error-rate (BER) formulation

The average received electrical SNR per subcarrier (γ) is given as [16]

$$\gamma = \frac{\left(\Re m G G_e n_{\text{T}} n_{\text{R}} G_{\text{T}} G_{\text{R}} P_{\text{T-av}}\left(\frac{\lambda}{4\pi L}\right)^2 \times 10^{(-\delta L/10)}\right)^2}{\langle i^2_{\text{shot}}\rangle+\langle i^2_{\text{ASE}}\rangle+\langle i^2_{\text{DB}}\rangle+\langle i^2_{\text{DS}}\rangle+\langle i^2_{\text{Th}}\rangle+\langle i^2_{\text{RIN}}\rangle}. \quad (33)$$

where G_e is the receiver amplifier gain, $\langle i^2_{\text{shot}}\rangle\left(=2eI_{\text{ph}}B_e\right)$ is the receiver-generated mean-square shot noise, I_{ph} is the primary photocurrent, e is electron charge and B_e is the receiver electrical bandwidth, $\langle i^2_{\text{ASE}}\rangle$ is the OA-generated mean-square shot noise which is the sum of shot-amplified spontaneous emission noise $\langle i^2_{\text{shot-ASE}}\rangle$ and the signal-amplified spontaneous emission noise $\langle i^2_{\text{S-ASE}}\rangle$, $\langle i^2_{\text{DB}}\rangle\,(=2eI_dG_eB_e)$ is the mean-square value of bulk dark current noise with dark current I_d, $\langle i^2_{\text{DS}}\rangle\,(=2eI_lG_eB_e)$ is the mean-square value of surface dark current noise with surface leakage current I_l, $\langle i^2_{\text{Th}}\rangle\left(=4G_e^2K_bTB_eF_n/R_L\right)$ is the mean-square value of thermal noise with receiver load R_L is receiver load, Boltzmann constant K_b, noise figure F_n, and absolute temperature T, $\langle i^2_{\text{RIN}}\rangle\,(=\text{RIN}I^2_{\text{ph}}B_e)$ is mean-square relative intensity noise with relative intensity noise RIN$(=-150\ \text{dB/Hz})$.

The performance of any communication system can be analyzed from the important metric known as bit error rate (BER) which can be defined as [54,57]

$$\begin{aligned}\mathrm{BER} &= \int_0^\infty P_e(h) f_h(h)\mathrm{d}h \\ &= \int_0^\infty P_e(h) \frac{(\alpha\beta)^{\frac{\alpha+\beta}{2}} h^{\frac{\alpha+\beta}{2}-1}}{\Gamma(\alpha)\Gamma(\beta) h_a^{\frac{\alpha+\beta}{2}}} G_{0,2}^{2,0}\left(\alpha\beta\frac{h}{h_a}\middle|_{\frac{\alpha-\beta}{2},\frac{\beta-\alpha}{2}}^{-}\right)\mathrm{d}h.\end{aligned} \tag{34}$$

where $P_e(h)$ is the conditional probability of error and for OFDM case it is given as [17]

$$\begin{aligned}P_e(h) &= \frac{2}{\log_2(M)} \\ &\times \left[\left(1-\frac{1}{\sqrt{M}}\right)\mathrm{erfc}\left(\sqrt{\frac{3\log_2(M)}{(M-1)}\frac{\gamma h^2}{2}}\right)\right].\end{aligned} \tag{35}$$

where γh^2 is the received instantaneous SNR, γ is the average end-to-end SNR.

According to [56, Eq. (06.27.26.0006.01)], the complementary error function in the form of MeijerG-function is $\mathrm{erfc}\left(\sqrt{X}\right) = \frac{1}{\sqrt{\pi}} G_{1,2}^{2,0}\left(X\middle|_{0,1/2}^{1}\right)$. Thus, The BER expression for M-QAM modulated OFDM-FSO link is defined as [17]

$$\begin{aligned}\mathrm{BER} &= \int_0^\infty P_e(h) \frac{(\alpha\beta)^{\frac{\alpha+\beta}{2}} h^{\frac{\alpha+\beta}{2}-1}}{\Gamma(\alpha)\Gamma(\beta) h_a^{\frac{\alpha+\beta}{2}}} G_{0,2}^{2,0}\left(\alpha\beta\frac{h}{h_a}\middle|_{\frac{\alpha-\beta}{2},\frac{\beta-\alpha}{2}}^{-}\right)\mathrm{d}h \\ &= \frac{2\left(1-\frac{1}{\sqrt{M}}\right)}{\sqrt{\pi}\log_2(M)} \int_0^\infty G_{1,2}^{2,0}\left(\frac{3\log_2(M)}{(M-1)}\frac{\gamma h^2}{2}\middle|_{0,1/2}^{-}\right) \\ &\times \frac{(\alpha\beta)^{\frac{\alpha+\beta}{2}} h^{\frac{\alpha+\beta}{2}-1}}{\Gamma(\alpha)\Gamma(\beta) h_a^{\frac{\alpha+\beta}{2}}} G_{0,2}^{2,0}\left(\alpha\beta\frac{h}{h_a}\middle|_{\frac{\alpha-\beta}{2},\frac{\beta-\alpha}{2}}^{-}\right)\mathrm{d}h.\end{aligned} \tag{36}$$

Let, $\left(\frac{\alpha\beta}{h_a}\right) = \omega$ and $\frac{\alpha+\beta}{2} = \varpi$. The product of two G-functions is also Meijer G function [58, Eq. (21)]. So, Eq. (36) is given as [17]

$$\begin{aligned}\mathrm{BER} &= \frac{\left(1-\frac{1}{\sqrt{M}}\right)}{\log_2(M)} \times \frac{2^{\alpha+\beta}}{\pi^{\frac{3}{2}}\Gamma(\alpha)\Gamma(\beta)} \\ &\times G_{5,2}^{2,4}\left(\frac{\frac{3\log_2(M)}{(M-1)}8\gamma h_a^2}{(\alpha\beta)^2}\middle|_{0,\frac{1}{2}}^{\frac{1-\alpha}{2},1-\frac{\alpha}{2},\frac{1-\beta}{2},1-\frac{\beta}{2},1}\right).\end{aligned} \tag{37}$$

5 Results and discussion

To analyze the performance of LoS and NLoS-FSO communication link, the value of different parameters is shown in Table 1. The achievable rates of various schemes versus SNR with ACO-OFDM technique is shown in Fig. 11. As the SNR increases, the achievable rate gap between PLNC and LoS scheme decreases quickly. From Eqs. (32) and (24), it can be seen that $\lim_{P\longrightarrow\infty} Ç^{\mathrm{PLNC}}/Ç^{\mathrm{LoS}} = 1$. At low SNR, there is an noticeable gap between $Ç^{\mathrm{PLNC}}$ and $Ç^{\mathrm{LoS}}$ which indicate that PLNC may not be the optimal scheme for low SNR. It is also clear that the performance of DNC scheme is not as good as that of PLNC scheme. From Eqs. (26) and (24), it can be seen that $Ç^{\mathrm{DNC}}/Ç^{\mathrm{LoS}} = 2/3$. Thus, the gap between achievable rates is 33% across all SNR. In case of TS and from Eqs. (25) and (24), it can be seen that $Ç^{\mathrm{TS}}/Ç^{\mathrm{LoS}} = 1/2$. Thus, the gap between achievable rates is 50% across all SNR. From the above discussion, it is clear that there is 100 and 33% throughput improvement with PLNC and DNC schemes, respectively compared to TS. ANC scheme does not give improved performance, as link-by-link channel-coded PLNC scheme gives, because of the noise is also amplified and transmitted to both the users node. 3T-ANC scheme gives improved performance compared to NLoS-TS, DNC, PLNC, ANC, and LoS scheme in both high- and low-SNR condition because, in addition with relay-assisted signal, there is direct signal also available at each node resulting into diversity gain. With MRC at each node, we can get the advantage of diversity and performance improvement as a result. With addition of diversity gain in performance 3T-ANC has no O/E/O conversion interface and electrical interface at the relay resulting in reduced cost and complexity. The achievable rate for PLNC, ANC, 3T-ANC schemes with ACO-OFDM technique are shown in Table 2. It is clear from this table that the performance gap for 3T-ANC relative to the PLNC scheme ranges from 38.4% at 15 dB to 36.5% at 20 dB SNR, respectively, and that for ANC ranges from 96.5% at 15 dB to 69% at 20 dB SNR, respectively.

The BER as a function of received power with ACO-OFDM technique for various network coding schemes is shown in Fig. 12. The performance of relay-assisted NLoS link, with PLNC scheme, is same as that of point-to-point LoS link. At BER of 10^{-3}, the received power with relay-assisted PLNC scheme is −20 dBm. For relay-assisted NLoS link with ANC scheme, the received power is −18.9 dBm and 1.1 dB degradation in receiver sensitivity as compared to PLNC scheme as a result. In the case of availability of both links, i.e., NLoS and LoS link, the receiver sensitivity is −26 dBm with 3T-ANC scheme. Thus there is 7.1 and 6 dB improvement in receiver sensitivity with 3T-ANC compared to ANC and PLNC scheme, respectively.

The comparison between the error performance of ACO-OFDM and 7 dB-biased DCO-OFDM FSO link is shown

Table 1 Parameters and their value

S. No.	Parameter	Value
1	Bit rate, R_b in Gb/s	1
2	Operating wavelength, λ in nm	1550
3	CP overhead, R_{cp}	1/9
4	modulation index, m	0.1
5	Total subcarriers	128
6	Pilot subcarriers	18
7	Data subcarriers	110
8	Gain of optical preamplifier, G in dB	20
9	Gain of receiver amplifier, G_e in dB	20
10	Noise figure of optical amplifier, F_n in dB	4.77
11	3-dB combined laser line width in MHz	5
12	Half beam divergence angle in μrad	72
13	Optical efficiency of transmitter	0.9
14	Optical efficiency of receiver	0.75
15	Aperture diameter of transmit laser in m	0.1
16	Aperture diameter of receive laser in m	0.3
17	Photodiode efficiency , η	0.75
18	Attenuation coefficient with visibility of 2 km in haze condition in (dB/km)	4
19	Optical window loss in dB	1
20	Atmospheric loss in strong turbulence in dB	13
21	System margin in dB	5
22	Pointing loss in dB	1
23	Refractive index structure parameter for strong atmospheric turbulence	5×10^{-14}
24	Modulation type	4-QAM

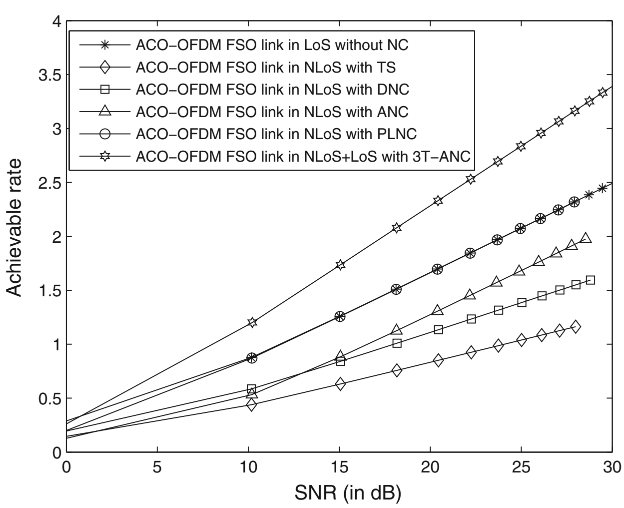

Fig. 11 Achievable rate versus SNR with various NC schemes

in Fig. 13. The results show that with 3T-ANC scheme, the ACO-OFDM technique is also power-efficient scheme where additional DC bias is not required to make the RF-OFDM signal positive. At BER of 10^{-3} with ACO-OFDM technique, there is about 2.7 and 3 dB improvement in receiver sensitivity in LoS and NLoS+LoS with 3T-ANC scheme compared to DCO-OFDM technique. Thus, the optical power budget for ACO-OFDM is higher compared to DCO-OFDM technique.

Table 2 Achievable rate with various NC scheme

SNR (dB)	PLNC	ANC	3T-ANC
15	1.25	0.88	1.73
20	1.67	1.28	2.28
25	2.08	1.68	2.84

In Figs. 14 and 15 the performance of C-FSO link with more than one relay nodes is analyzed. The error performance of C-FSO link is improved with two relay nodes. One can observe that with increasing number of relay there is improvement in performance. However, the improvement is marginal for more than two number of relays, because each relay amplify the noise also. The increased number of relays can also increase the cost and complexity of the relay-assisted C-FSO link.

From the above discussion it is clear that relay-assisted NLoS link can make a continuous information exchange, even if LoS is breakdown between two users, but at the cost

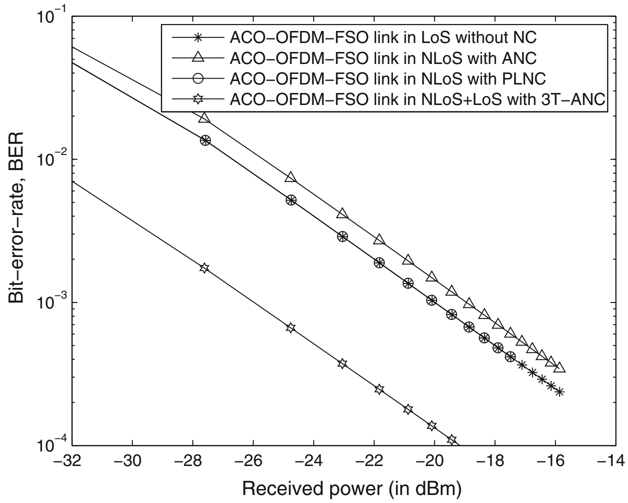

Fig. 12 BER versus received power with various NC schemes

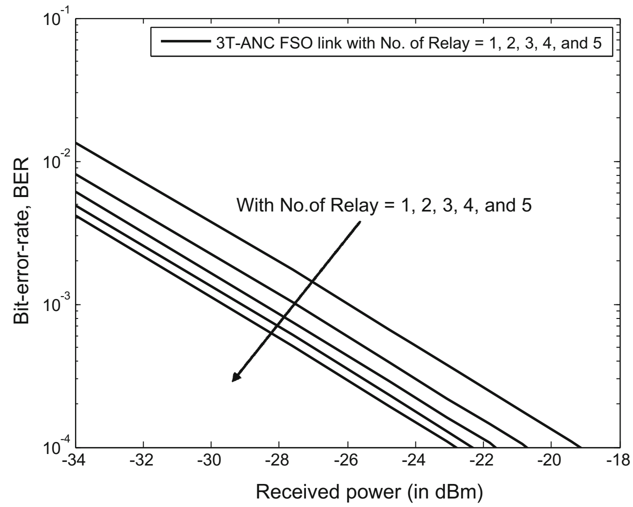

Fig. 14 BER versus received power of multiple relayed 3T-ANC FSO link

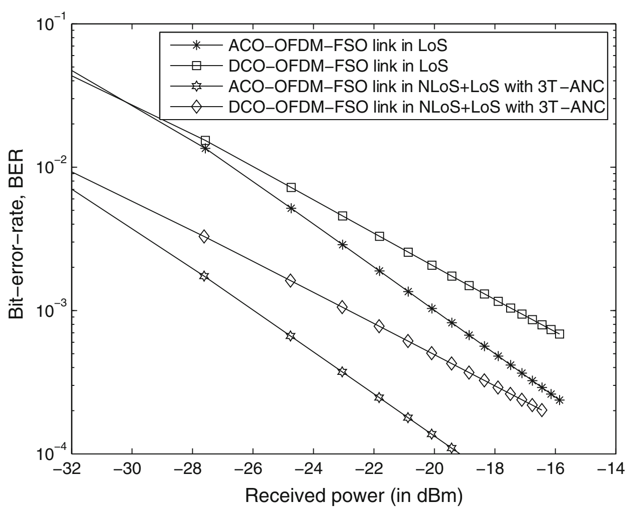

Fig. 13 BER versus received power with ACO/DCO-OFDM FSO link

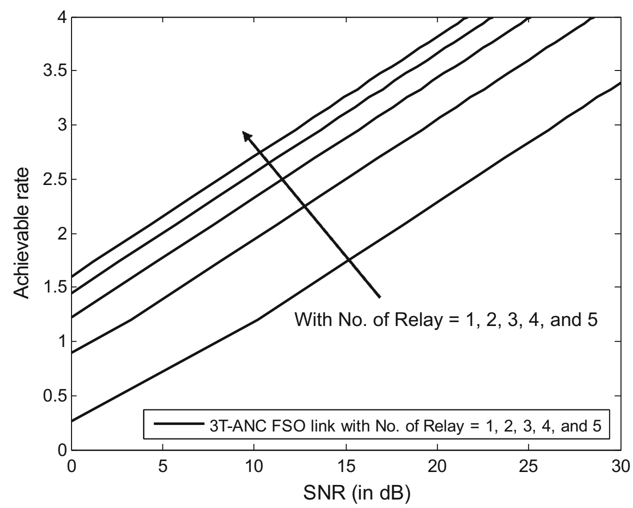

Fig. 15 Achievable rate versus SNR with multiple relay

of reduced achievable rate and error performance. PLNC gives better performance in NLoS condition but with expensive OER relay which require O/E/O conversion resulting in increased complexity at relay. ANC allow the use of cost-effective OR relay where O/E/O is not required resulting in reduced complexity and energy saving at the relay but performance is degraded since the noise is also amplified at the relay. On the other hand, when NLoS as well as direct LoS links are available, ANC with three time slot known as 3T-ANC gives improved performance compared to PLNC with energy saving and reduced cost and complexity. We have also shown that the optical power budget for ACO-OFDM is higher compared to DCO-OFDM technique. To further improve the performance C-FSO link with multiple relay nodes can be used, but with more than two relay nodes, there is marginal improvement as relay also amplify the noise in the link.

6 Conclusion

OFDM technique gives improved performance in FSO link because of its dispersion tolerance capacity, efficient utilization of electrical bandwidth, ease of channel and phase estimation, and scalability to higher-order modulation. The ACO-OFDM technique is more optical power efficient compared to DCO-OFDM as ACO-OFDM signal eliminates the need of an additional DC bias to make it unipolar. FSO link requires LoS condition between two users and in NLoS condition communication between them will breakdown. In this situation, to continue information exchange between two users with increased achievable rate and improved error performance, we have proposed the use of OR relay-assisted link with 3T-ANC scheme. Analytical results shows that PLNC gives better performance in NLoS condition but with expensive OER relay. ANC allow the use of cost-effective energy-saving relay but at the cost of performance degradation as noise is also amplified at the relay. On the other hand, when NLoS as well as direct LoS links are available, 3T-ANC gives improved performance compared to PLNC with energy saving, reduced, cost and complexity at the relay node. The C-FSO link with multiple relay nodes can be used to further improve the error performance of the link, but with more than two relay nodes, there is marginal improvement as relay also amplify the noise in the link.

References

[1] Kazaura, K., Wakamori, K., Matsumoto, M., Higashino, T., Tsukamoto, K., Komaki, S.: RoFSO: a universal platform for convergence of fiber and free-space optical communication networks. IEEE Comm. Mag. **48**(2), 130–137 (2010). doi:10.1109/MCOM.2010.5402676

[2] Tsukamoto, K., Hashimoto, A., Aburakawa, Y., Matsumoto, M.: The case for free space. IEEE Microw. Mag. **10**(5), 84–92 (2009). doi:10.1109/MMM.2009.933086

[3] Bekkali, A., Dat, P.T., Kazaura, K., Wakamori, K., Matsumoto, M., Higashino, T., Tsukamoto, K., Komaki, S.: Performance evaluation of an advanced DWDM RoFSO system for transmitting multiple RF signals. IEICE Trans. Fundam. Electron. Commun. Comput.Sci. **92**(11), 2697–2705 (2009)

[4] Akbulut, A., Efe, M., Ceylan, A.M., Ari, F., Telatar, Z., Ilk, H.G., Tugac, S.: An experimental hybrid FSO/RF communication system. In: Proceedings of the IASTED International Conference on Communication System and Networks, CSN 2003, Benalmdena, Spain pp. 406–411 (2003)

[5] Vaiopoulos, N., Sandalidis, H.G., Varoutas, D.: WiMAX on FSO: outage probability analysis. IEEE Trans. Commun. **60**(10), 2789–2795 (2012). doi:10.1109/TCOMM.2012.071212.110182

[6] Cvijetic, N., Wilson, S.G.: OPN01-4: WiMAX access using optical wireless technology with heterodyne detection in turbulent atmospheric channels. IEEE Globecom **2006**, 1–5 (2006). doi:10.1109/GLOCOM.2006.361

[7] Cvijetic, N., Wang, T.: WiMAX over free-space optics—evaluating OFDM multi-subcarrier modulation in optical wireless channels. In: Sarnoff Symposium, 2006 IEEE, pp. 1–4 (2006). doi:10.1109/SARNOF.2006.4534760

[8] Cvijetic, N., Wang, T.: A MIMO Architecture for IEEE 802.16d (WiMAX) Heterogeneous wireless access using optical wireless technology. In: Koucheryavy, Y., Harju, J., Iversen, V.B. (eds.) Next Generation Teletraffic and Wired/Wireless Advanced Networking: Proceedings of 6th International Conference, NEW2AN 2006, St. Petersburg, Russia, May 29–June 2, 2006, pp. 441–451. Springer, Berlin (2006). doi:10.1007/11759355_40

[9] Cvijetic, N., Qian, D., Wang, T.: 10Gb/s free-space optical transmission using OFDM. In: Optical Fiber communication/National Fiber Optic Engineers Conference, 2008. OFC/NFOEC 2008, pp. 1–3. doi:10.1109/OFC.2008.4528442

[10] Zdravkovi, N., Petkovic, M.I., Djordjevic, G.T., Kansanen, K.: Outage analysis of mixed FSO/WiMAX link. IEEE Photonics J. **8**(1), 1–14 (2016). doi:10.1109/JPHOT.2016.2516250

[11] Bekkali, A., Naila, C.B., Kazaura, K., Wakamori, K., Matsumoto, M.: Transmission analysis of OFDM-based wireless services over turbulent radio-on-FSO links modeled by Gamma–Gamma distribution. IEEE Photonics J. **2**(3), 510–520 (2010). doi:10.1109/JPHOT.2010.2050306

[12] Sharma, M., Chadha, D., Chandra, V.: Performance analysis of spatially multiplexed MIMO-OFDM free space optical communication system. In: 2014 International Conference on Signal Processing and Communications (SPCOM), pp. 1–5 (2014). doi:10.1109/SPCOM.2014.6983942

[13] Sharma, M., Chadha, D., Chandra, V.: Capacity evaluation of MIMO-OFDM free space optical communication system. In 2013 Annual IEEE India Conference (INDICON), pp. 1–4 (2013). doi:10.1109/INDCON.2013.6726078

[14] Bai, F., Su, Y., Sato, T.: Performance evaluation of a dual diversity reception base on OFDM RoFSO systems over correlated log-normal fading channel. In: Proceedings of the 2014 ITU Kaleidoscope Academic Conference: Living in a converged world - Impossible without standards?, pp. 263–268 (2014). doi:10.1109/Kaleidoscope.2014.6858473

[15] Wang, Y., Wang, D., Ma, J.: On the performance of coherent OFDM systems in free-space optical communications. IEEE Photonics J. **7**(4), 1–10 (2015). doi:10.1109/JPHOT.2015.2450532

[16] Kumar, P., Srivastava, A.: Enhanced performance of FSO link using OFDM and comparison with traditional TDM-FSO link. In: IEEE International Broadband and Photonics (IBP) Conference, Bali, Indonesia, pp. 1–6 (2015). doi:10.1109/ANTS.2013.6802858

[17] Kumar, P., Srivastava, A.: Performance improvement of OFDM-FSO multi-user communication system with combined transmit frequency diversity and receive space diversity. Optics Communications **366**, 410–418 (2016). doi:10.1016/j.optcom.2015.12.059. http://www.sciencedirect.com/science/article/pii/S0030401815303928

[18] Nee, R.V., Prasad, R.: OFDM for Wireless Multimedia Communications, 1st edn. Artech House Inc, Norwood (2000)

[19] Shieh, W., Djordjevic, I.: Orthogonal frequency division multiplexing for optical communications. Academic Press, Cambridge (2010)

[20] Gonzalez, O., Perez-Jimenez, R., Rodriguez, S., Rabadan, J., Ayala, A.: Adaptive OFDM system for communications over the indoor wireless optical channel. IEE Proc. Optoelectron. **153**(4), 139–144 (2006). doi:10.1049/ip-opt:20050081

[21] Armstrong, J., Schmidt, B.J.C., Kalra, D., Suraweera, H.A., Lowery, A.J.: SPC07-4: performance of asymmetrically clipped optical OFDM in AWGN for an intensity modulated direct detection system. IEEE Globecom **2006**, 1–5 (2006). doi:10.1109/GLOCOM.2006.571

[22] Wilson, S.K., Armstrong, J.: Digital modulation techniques for optical asymmetrically-clipped OFDM. In: 2008 IEEE Wireless Communications and Networking Conference, pp. 538–542 (2008). doi:10.1109/WCNC.2008.100

[23] Dissanayake, S.D., Armstrong, J.: Comparison of ACO-OFDM, DCO-OFDM and ADO-OFDM in IM/DD systems. J. Lightwave Technol. **31**(7), 1063–1072 (2013). doi:10.1109/JLT.2013.2241731

[24] Ranjha, B., Kavehrad, M.: Hybrid asymmetrically clipped OFDM-based IM/DD optical wireless system. IEEE/OSA J. Opt. Commun. Netw. **6**(4), 387–396 (2014). doi:10.1364/JOCN.6.000387

[25] Wu, N., Bar-Ness, Y.: A novel power-efficient scheme asymmetrically and symmetrically clipping optical (ASCO)-OFDM for IM/DD optical systems. EURASIP J. Adv. Signal Process. **2015**(1), 3 (2015). doi:10.1186/1687-6180-2015-3

[26] Gui, T., Li, C., Yang, Q., Xiao, X., Meng, L., Li, C., Yi, X., Jin, C., Li, Z.: Auto bias control technique for optical OFDM trans-

mitter with bias dithering. Opt. Express **21**(5), 5833–5841 (2013). doi:10.1364/OE.21.005833
[27] Zhang, M., Zhang, Z.: An optimum DC-biasing for DCO-OFDM system. IEEE Commun. Lett. **18**(8), 1351–1354 (2014). doi:10.1109/LCOMM.2014.2331068
[28] Armstrong, J., Schmidt, B.J.C.: Comparison of asymmetrically clipped optical OFDM and DC-biased optical OFDM in AWGN. IEEE Commun. Lett. **12**(5), 343–345 (2008). doi:10.1109/LCOMM.2008.080193
[29] Patel, D., Singh, V.K., Dalal, U.D.: Assessment of the DC bias to mitigate the clipping noise in DCO-OFDM, ACO-OFDM; and non-linear distortion of DFB laser transmitted through dispersive single mode fibers in IM/DD Systems. Wirel. Pers. Commun., 1–20 (2017). doi:10.1007/s11277-017-4170-y
[30] Chen, L., Krongold, B., Evans, J.: Theoretical characterization of nonlinear clipping effects in IM/DD optical OFDM systems. IEEE Trans. Commun. **60**(8), 2304–2312 (2012). doi:10.1109/TCOMM.2012.060112.110136
[31] Bohren, C., Huffman, D.: Absorption and Scattering of Light by Small Particles. Wiley, New York (2008). https://books.google.co.in/books?id=ib3EMXXIRXUC
[32] El-Shimy, M.A.E.H.: Communications Through Non-Line-of-Sight Solar-Blind Ultraviolet Scattering Channels. McMaster University, Hamilton (2014). http://hdl.handle.net/11375/16231
[33] Kolka, Z., Biolek, D., Biolkova, V.: Simulation of atmospheric optical channel with ISI. In: Proceedings of the 8th WSEAS International Conference on Circuits, Systems, Electronics, Control & Signal Processing, CSECS'09, pp. 198–201. World Scientific and Engineering Academy and Society (WSEAS), Stevens Point (2009). http://dl.acm.org/citation.cfm?id=1736282.1736317
[34] Kumar, P., Srivastava, A.: Receiver sensitivity improvement of OFDM-FSO link using SRM device. In: 2015 IEEE International Conference on Advanced Networks and Telecommuncations Systems (ANTS), pp. 1–6(2015). doi:10.1109/ANTS.2015.7413645
[35] Kumar, N., Teixeira, A.L.J.: 10 Gbit/s OFDM based FSO communication system using M-QAM modulation with enhanced detection. Opt. Quantum Electron. **48**(1), 1–7 (2015). doi:10.1007/s11082-015-0272-5
[36] Sharma, V., Kumar, N.: Improved analysis of 2.5 Gbps-inter-satellite link (ISL) in inter-satellite optical-wireless communication (IsOWC) system. Opt. Commun. **286**, 99–102 (2013). doi:10.1016/j.optcom.2012.08.055. http://www.sciencedirect.com/science/article/pii/S0030401812009030
[37] Liew, S.C., Zhang, S., Lu, L.: Physical-layer network coding: Tutorial, survey, and beyond. Phys. Commun. **6**, 4–42 (2013). doi:10.1016/j.phycom.2012.05.002. http://www.sciencedirect.com/science/article/pii/S1874490712000419. Network Coding and its Applications to Wireless Communications
[38] Abu-Almaalie, Z., Ghassemlooy, Z., Le-Minh, H., Aslam, N.: Physical layer network coding with two-way relay free space optical communication link. In: 2015 Internet Technologies and Applications (ITA), pp. 292–297 (2015). doi:10.1109/ITechA.2015.7317412
[39] He, F., Chen, X., Xiao, L., Zhou, S.: Low complexity power allocation for two-way decode-and-forward OFDM relay networks. In: 2016 IEEE/CIC International Conference on Communications in China (ICCC), pp. 1–6 (2016). doi:10.1109/ICCChina.2016.7636718
[40] Huang, G., Tang, D.: Wireless information and power transfer in two-way OFDM amplify-and-forward relay networks. IEEE Commun. Lett. **20**(8), 1563–1566 (2016). doi:10.1109/LCOMM.2016.2570751
[41] Trinh, P.V., Thang, T.C., Pham, A.T.: Two-way all-optical AF relaying FSO systems over Malaga (M) channels with pointing errors. In 2016 IEEE International Conference on Communications (ICC), pp. 1–7 (2016). doi:10.1109/ICC.2016.7511176
[42] Ezzine, S., Abdelkefi, F., Cances, J.P., Meghdadi, V., Bouallgue, A.: Channel capacity and SA-BER performances evaluation of an OFDM-based two-way relaying AF-PNC-PLC systems. In: 2016 IEEE 30th International Conference on Advanced Information Networking and Applications (AINA), pp. 39–46 (2016). doi:10.1109/AINA.2016.150
[43] Katti, S., Gollakota, S., Katabi, D.: Embracing wireless interference: analog network coding. In: Proceedings of the 2007 Conference on Applications, Technologies, Architectures, and Protocols for Computer Communications, SIGCOMM '07, pp. 397–408. ACM, New York (2007). doi:10.1145/1282380.1282425
[44] Gacanin, H., Adachi, F.: Broadband analog network coding. IEEE Trans. Wirel. Commun. **9**(5), 1577–1583 (2010). doi:10.1109/TWC.2010.05.091053
[45] Sjodin, T.: A channel estimation scheme for analog network coding based on OFDM in multipath fading environment (2009). http://www8.cs.umu.se/education/examina/Rapporter/TomasSjodin.pdf
[46] Yadav, S., Upadhyay, P.: Impact of outdated channel estimates on opportunistic two-way ANC-based relaying with three-phase transmissions. IEEE Trans. Veh. Technol. **64**(12), 5750–5766 (2015). doi:10.1109/TVT.2014.2387480
[47] Park, J.C., Song, I., Kim, Y.H.: Outage-optimal allocation of relay power for analog network coding with three transmission phases. IEEE Commun. Lett. **16**(6), 838–841 (2012). doi:10.1109/LCOMM.2012.041112.120094
[48] Wang, J.S., Lee, S.R., Kim, Y.H.: Rate-aware three phase analog network coding with low-complexity multi-antenna relay processing. In Wireless Communications and Networking Conference (WCNC), 2014 IEEE, pp. 1065–1069 (2014). doi:10.1109/WCNC.2014.6952276
[49] Park, J.C., Wang, J.S., Kim, Y.H.: Rate and outage performance of non-regenerative two-way relaying protocols with direct link. In: Vehicular Technology Conference (VTC Fall), 2011 IEEE, pp. 1–5 (2011). doi:10.1109/VETECF.2011.6093190
[50] Zhang, S., Liew, S.C., Lu, L.: Schemes, physical layer network coding, over finite and infinite fields. In: Global Telecommunications Conference. IEEE GLOBECOM 2008. IEEE, pp. 1–6 (2008). doi:10.1109/GLOCOM.2008.ECP.726
[51] Arnon, S.: Encyclopedia of optical engineering. In: Driggers, R.G., Hoffman, C., Driggers, R. (eds.) Optical Wireless Communications, pp. 1866–1886. CRC Press, Boca Raton (2003)
[52] Vaiopoulos, N., Sandalidis, H., Varoutas, D.: Using a HAP network to transfer WiMAX OFDM signals: outage probability analysis. IEEE/OSA J. Opt. Commun. Netw. **5**(7), 711–721 (2013). doi:10.1364/JOCN.5.000711
[53] Al-Raweshidy, H., Komaki, E.E.S.: Radio Over Fiber Technology for Mobile Communication Networks. Artech House, Norwood (2002)
[54] Kaur, P., Jain, V.K., Kar, S.: Performance analysis of FSO array receivers in presence of atmospheric turbulence. IEEE Photonics Technol. Lett. **26**(12), 1165–1168 (2014). doi:10.1109/LPT.2014.2316534
[55] Ghassemlooy, Z., Popoola, W., Rajbhandari, S.: Optical Wireless Communications: System and Channel Modelling with MATLAB, Optical Wireless Communications: System and Channel Modelling with MATLAB, 1st edn. CRC Press Inc, Boca Raton (2012)
[56] Wolfram function site (2009). http://functions.wolfram.com/PDF/MeijerG.pdf
[57] Song, X., Yang, F., Cheng, J.: Subcarrier intensity modulated optical wireless communications in atmospheric turbulence with pointing errors. IEEE/OSA J. Opt. Commun. Netw. **5**(4), 349–358 (2013). doi:10.1364/JOCN.5.000349
[58] Adamchik, V.S., Marichev, O.I.: The algorithm for calculating integrals of hypergeometric type functions and its realization in

reduce system. In: Proceedings of the International Symposium on Symbolic and Algebraic Computation, ISSAC '90, pp. 212–224. ACM, New York (1990). doi:10.1145/96877.96930

Pravindra Kumar received his B.Tech degree from U.P.Tech., University, Lucknow, India. He received his M.Tech degree in digital communication from G.G.S.I. P. University, New Delhi, India. He has submitted his Ph.D. Thesis in the School of Computing and Electrical Engineering (SCEE) at Indian Institute of Technology Mandi, Mandi (H.P), India. His research interest on OFDM-based Optical Core and Access Networks, Long Reach PONs, Optical Wireless Communication Systems, Li-Fi Technology, Optical Signal Processing, Analog Network Coding.

Satyajit Thakor received his B.Eng. in Electronics and Telecommunication from Dr. B. A. M. University, India in 2004. He received his M.Eng. and PhD in Telecommunications in 2006 and 2012 from University of South Australia. He was a postdoctoral fellow at Institute of Network Coding, Chinese University of Hong Kong from 2011 to 2014. Since January 2014, he is an Assistant Professor in School of Computing and Electrical Engineering at Indian Institute of Technology Mandi. Dr. Satyajit Thakor was a recipient of Michael Miller Medal 2012 for his Ph.D. thesis and the Endeavour Research fellowship 2009. His research interests include information theory, network coding, and distributed storage.